Chemistry & Biology 13, 1091–1100, October 2006 ©2006 Elsevier Ltd All rights reserved DOI 10.1016/j.chembiol.2006.08.011

Global Effects of Mistranslation from an Editing Defect in Mammalian Cells

Leslie A. Nangle,[1] Candace M. Motta,[1] and Paul Schimmel[1,*]
[1] Departments of Molecular Biology and Chemistry and The Skaggs Institute for Chemical Biology
The Scripps Research Institute
10550 North Torrey Pines Road
La Jolla, California 92037

Summary

Aminoacyl-tRNA synthetases prevent mistranslation, or genetic code ambiguity, through specialized editing reactions. Mutations that disrupt editing in bacteria adversely affect cell growth and viability, and recent work in the mouse supports the idea that translational errors caused by an editing defect lead to a neurological disease-like phenotype. To further investigate the connection of mistranslation to cell pathology, we introduced an inducible transgene expressing an editing-deficient valyl-tRNA synthetase into mammalian cells. Introducing mistranslation precipitated a disruption of cell morphology and membrane blebbing, accompanied by activation of caspase-3, consistent with an apoptotic response. Addition of a noncanonical amino acid that is misactivated, but not cleared, by the editing-defective enzyme exacerbated these effects. A special ambiguity-detecting sensor provided direct readout of mistranslation in vivo, supporting the possibility that decreased translational fidelity could be associated with disease.

Introduction

Connections between specific human diseases and aminoacyl-tRNA synthetases (AARSs) illustrate the emerging awareness of the importance of these enzymes in disease pathology [1, 2]. Although the mechanism of disease causation is not known, we hypothesize that defects in activities idiosyncratically associated with specific synthetases, such as editing, could be responsible for pathological mutations. In a related vein, potential links between faulty translation and disease have been reported for specific translation factors. For example, levels of the translation initiation factor eIF-4E are elevated in human cancers and are linked to conversion of cells into malignant states in culture [3–5]. In one study, NIH/3T3 cells exhibited a transformed phenotype after overexpression of eIF-4E. Tumors developed when the transformed cell lines were injected into nude mice. In another investigation, profound neuromuscular problems were observed in mice that carry a deleterious mutation in translation elongation factor eEF1A2 [6–8]. Recently, protein synthesis was again highlighted in the human neurodegenerative disease VWM/CACH (vanishing white matter/childhood ataxia with central hypomyelination). This disease is connected to mutations in translation factor eIF-2B [9, 10].

These examples illustrate that maintaining control, and possibly fidelity, in translation may be far more sensitive and subtle than previously thought. With that in mind, we sought to determine whether inducing mistranslation via mutation of a component of the translation apparatus, i.e., an aminoacyl-tRNA synthetase, could be connected to an apparent phenotype in mammalian cells. Many tRNA synthetases have editing activities to correct errors of aminoacylation and prevent mistranslation, or genetic code ambiguity [11–13]. At least in bacterial cells, these activities are critical for optimal cell growth and, under some circumstances, cell viability [14, 15]. Thus, disruption of tRNA synthetase editing functions may also have broad consequences in mammalian cells. The significance of the editing function traces back to the highly accurate genetic code algorithm relating each amino acid to specific nucleotide triplets found in messenger RNAs (mRNAs). This algorithm is established in aminoacylation reactions catalyzed by AARSs, in which each amino acid is linked to the 2′ or 3′ OH of the cognate tRNA that bears the anticodon triplet of the code that corresponds to the attached amino acid [16–18]. To maintain high accuracy levels [13, 19, 20], certain AARSs that are forced to discriminate between sterically similar amino acids have a second active site that clears, or edits, incorrectly charged amino acids [21–24]. If a mutation affects the editing function of one of these enzymes, production of mischarged tRNAs results in misincorporation of amino acids that can, in principle, create pools of statistical, heterogeneous proteins [25–27].

Recently, mice harboring a single missense mutation in the editing domain of alanyl-tRNA synthetase (AlaRS) were shown to exhibit severe ataxia accompanied by degeneration of Purkinje cells in the brain [28]. The mutation in murine AlaRS produced a partial defect in the ability of the enzyme to clear mischarged Ser-tRNA^{Ala} in vitro. Although the editing defect was only partial, a strong phenotype was seen in the mouse. In particular, ataxia and Purkinje cell degeneration were accompanied by the upregulation of cytoplasmic protein chaperones and induction of the unfolded protein response.

Here, we report results of a laboratory-based system to directly study mistranslation within mammalian cells that harbor an editing-deficient tRNA synthetase. We chose a different enzyme that has a potent activity for preventing mistranslation, ValRS. This choice enabled us to investigate whether the kind of effects seen in mouse were idiosyncratic to AlaRS or more general. Also, by working with a mammalian cell system in culture, we could more closely control the production of the editing-defective enzyme and set up a specialized system to give a direct readout of mistranslation. The results obtained support the hypothesis that pathological states can arise from mistranslation in mammalian cells, caused by a single missense mutation in the editing domain of a tRNA synthetase and, in addition, that such mutations can dominate over the wild-type allele.

*Correspondence: schimmel@scripps.edu

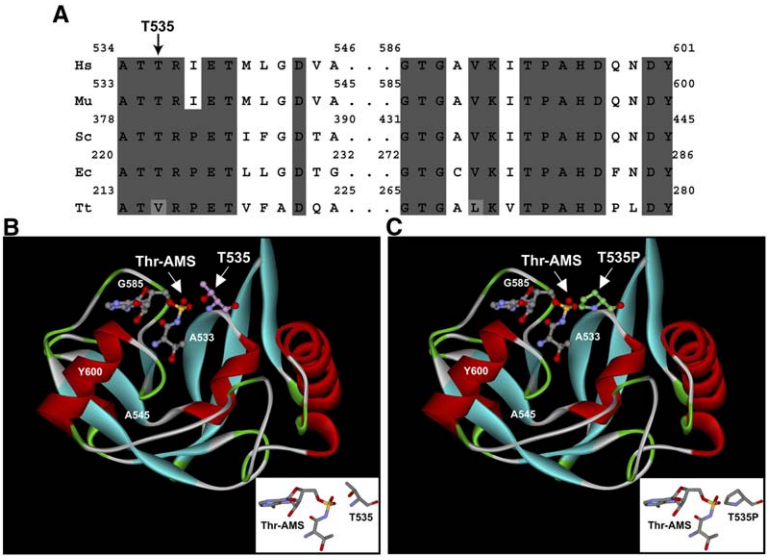

Figure 1. Modeling of a Mutated Residue within the Editing Domain of *M. musculus* ValRS

(A) Alignment of residues in the editing site of ValRS from *Homosapiens* (Hs), *Mus musculus* (Mu), *Saccharomyces cerevisiae* (Sc), *Escherichia coli* (Ec), and *Thermus thermophilus* (Tt). Highly conserved residues are shaded in dark gray; light-gray shading indicates isosteric residues at conserved sites. The arrow indicates the location of mutated T in ValRS.

(B) Model of the editing domain of *M. musculus* ValRS created by 3D-PSSM based on the structure of *T. thermophilus* ValRS highlighting the location of T535. Residues are indicated with *M. musculus* numbering. Inset: T535 proximity to the bound Thr-AMS analog.

(C) Modeling the T535P substitution onto the editing domain of *M. musculus* ValRS. Inset: Proximity change of T535P to the bound Thr-AMS analog.

Moreover, the severity of the cellular response appears to be correlated with the degree of mistranslation that is induced.

Results

Structural Implications for Creating Editing-Deficient ValRS

The editing reaction of ValRS occurs at a distinct second active site located in an insertion, the connective polypeptide 1 (CP1), that is conserved throughout archaea, bacteria, and eukaryotes [29–31]. Point mutations in CP1 of *Escherichia coli* ValRS render the enzyme incapable of efficient hydrolysis of mischarged tRNAs, such as Thr-tRNA^{Val}, which are then released for mRNA decoding [15, 25]. At the same time, presumably because the site for editing is distal to the active site for aminoacylation, these editing-defective mutants are fully competent for aminoacylation. In the presence of a *ΔvalS* null background in *E. coli*, each tested editing-defective mutant ValRS adversely affected bacterial cell viability when cells were grown in the presence of elevated amounts of a noncognate amino acid that is misactivated by ValRS (i.e., Thr, L-α-aminobutyric acid [α-Abu]). The magnitude of the editing defect measured in vitro directly correlated with the degree of sensitivity to noncognate amino acid addition that was observed in vivo.

T222P *E. coli* ValRS was the most editing defective of the previously studied enzymes. Significantly, T222 in *E. coli* ValRS is highly conserved through evolution (Figure 1A). (Of the available ValRS sequences, only a few bacterial species, including *Thermus thermophilus* and some species of *Deinococcus*, have replaced this highly conserved T with the isosteric V. Interestingly, T also appears at this position in other class I editing-proficient aminoacyl-tRNA synthetases [IleRS and LeuRS] that contain the CP1 insertion [32, 33].) Recently, the structure of the *T. thermophilus* ValRS editing domain complexed with a Thr-AMP analog (N-[L-threonyl]sulfamoyl)adenosine was solved [34]. This structure provided the opportunity to rationalize the severe phenotype of the T222P substitution in *E. coli* ValRS, and to visualize the corresponding substitution in a mammalian ValRS (T535P *Mus musculus* ValRS), indicating its potential effects on hydrolytic editing. Using the structure of the *T. thermophilus* CP1 insertion as a scaffold, a model of the *M. musculus* ValRS [35] active site for editing was generated by homology modeling by using the program 3D-PSSM (three-dimensional position-specific scoring matrix) [36, 37]. Side chains were constructed with SCWRL [38]. A PSSM E-value of 0.00339 was assigned to the model and indicated >95% confidence in the prediction. In this model, a T is placed at the position corresponding to T535 in *M. musculus* ValRS, replacing V214 in *T. thermophilus* ValRS (Figure 1B). In this model, the residue corresponding to T535 is close to the bound Thr-AMS and helps to form the binding pocket for the misactivated adenylate or the threonyl moiety of Thr-tRNA^{Val}. When a P replaces T535, assuming no structural rearrangement, the misactivated substrate is partly occluded (Figure 1C). (More likely, the introduced P would produce a significant distortion of the binding pocket.) This analysis provided a structural rationale for the potency of the previously studied T222P substitution of *E. coli* ValRS and supported the idea that a similar substitution in *M. musculus* ValRS would be deleterious to editing.

Initial Characterization of T535P *M. musculus* ValRS

Wild-type and T535P *M. musculus* ValRS were overexpressed in *E. coli*, isolated, and assayed for aminoacylation activity. Both proteins were functional for aminoacylation (Figure 2A) of bulk mammalian tRNA isolated from bovine liver. That the aminoacylation activities of these enzymes were similar shows that introduction of the T535P mutation introduced no large-scale structural changes that would interfere with the active site for aminoacylation. This result is consistent with prior work with the *E. coli* ortholog and further established that the two active sites, separated by ~30 Å, are functionally independent.

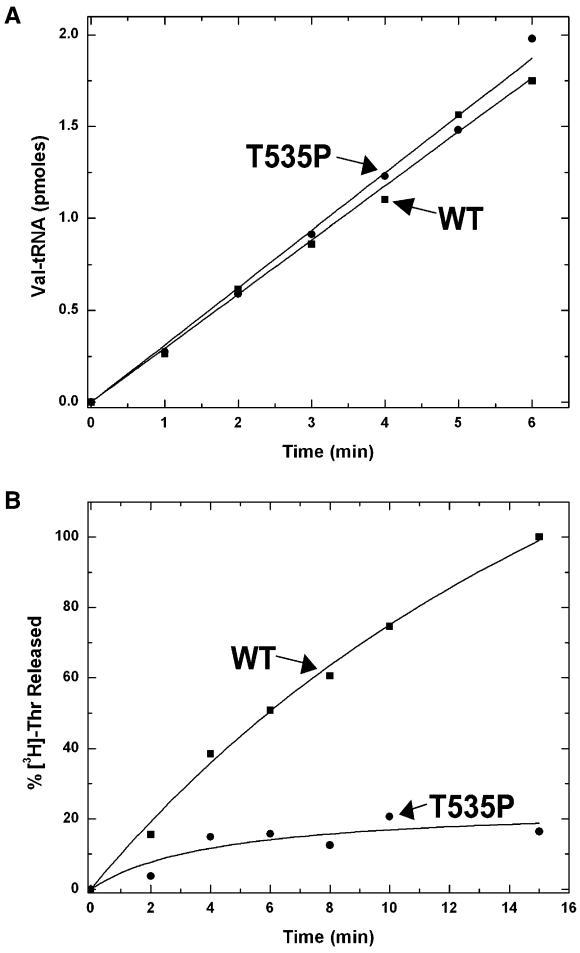

Figure 2. T535P ValRS Is Deficient in Editing, but Not Aminoacylation (A and B) (A) Aminoacylation of tRNA with valine and (B) deacylation of misacylated [^{3}H]-Thr-tRNA^{Val} by WT and T535P ValRS. Results are representative of means from three independent experiments.

Next, the ability of wild-type and T535P ValRS to hydrolyze Thr-tRNA^{Val} was investigated (Figure 2B). For this purpose, the necessary large amounts of pure [^{3}H]-Thr-tRNA^{Val} were generated by using *E. coli* T222P ValRS to mischarge endogenous purified *E. coli* tRNA^{Val} (for reasons of technical constraints and convenience, mammalian Thr-tRNA^{Val} was not prepared). While *E. coli* tRNA^{Val} is a poor substrate for aminoacylation by *M. musculus* ValRS, the mammalian enzyme can still distinguish Thr from Val in the context of *E. coli* tRNA^{Val} and can hydrolyze mischarged Thr-tRNA^{Val}, as was observed for the wild-type enzyme here. (A similar lack of preference in tRNA selection by the hydrolytic editing site has also been observed for PheRS from *Saccharomyces cerevisiae*. In this case, the cytoplasmic PheRS cannot aminoacylate mitochondrial tRNA^{Phe}, yet it readily deacylates mischarged mitochondrial Tyr-tRNA^{Phe} in *trans* [39].) In contrast, T535P ValRS was severely compromised for clearing Thr-tRNA^{Val}. Thus, as seen for the *E. coli* enzyme, the T → P substitution at the analogous position in ValRS greatly reduced its hydrolytic editing activity.

Expression of Wild-Type and Editing-Defective ValRS in Mammalian Cells

To test the effects of a ValRS editing deficiency in vivo, an inducible transgene of both wild-type and T535P ValRS was constructed. Mammalian ValRS, like other AARSs of higher eukaryotes, has additional domains that are appended to the highly conserved core enzyme that is the ortholog of prokaryotic ValRSs [40, 41] (the core itself has ~32 % sequence similarity between *E. coli* and *M. musculus* ValRS). These additional domains are dispensable (for aminoacylation) and are contained within a 295 amino acid polypeptide fused to the N-terminal side of the core enzyme [42–46]. Treatment with elastase selectively cleaves ~250 amino acids from the N-terminal side of full-length human ValRS [44, 46], suggesting that, under some circumstances, a truncated form may occur naturally in mammalian cells. The most N-terminal of these appended domains is unique to ValRSs of higher eukaryotes and is required to facilitate the formation of a 5 subunit 700 kDa complex between ValRS and elongation factor 1H [44, 47, 48]. In addition to aminoacylation activity, this complex functions in translation to sustain mRNA-dependent polypeptide synthesis in the presence of EF-2 and mRNA-dependent binding of charged tRNA to ribosomes. Because cells specifically expressing T535P (but not wild-type) ValRS were unstable, the transgene was constructed to encode a protein in which residues 1–295 were removed from the N terminus to create ValRS$^{\Delta}$ (a transgene similar to that used by Park et al. to overexpress human ValRS in HEK293 cells [49]), thereby allowing us to generate mischarged tRNA^{Val} in mammalian cells. We speculate that, with full-length T535P ValRS, Thr-tRNA^{Val} is more efficiently transferred to the EF-1H complex and the ribosome than is the case with the T535P ValRS$^{\Delta}$. This increase in efficiency would result in more mistranslation and greater toxicity.

Constructs encoding wild-type and T535P mutant ValRS$^{\Delta}$ were transfected into NIH/3T3 mouse fibroblast cells and, after induction for 24 hr, yielded soluble protein. Stably transfected cell lines capable of expressing each of the constructs were generated, with both transgene constructs yielding a single cell line. Production of recombinant ValRS$^{\Delta}$ in these cell lines was dependent on induction by mifepristone (MFP), and there was no basal expression detectable (by western blot) in the absence of MFP (Figure 3A). The cell lines encoding wild-type and T535P ValRS$^{\Delta}$ expressed protein at similar levels, with slightly more ValRS$^{\Delta}$ seemingly produced in the wild-type cell line at the same concentration of the MFP inducer.

Introduction of an Editing-Deficient ValRS$^{\Delta}$ Transgene Disrupts Mammalian Cell Morphology in a Manner Exacerbated by α-Abu

Prolonged induction of the stably transfected NIH/3T3 cell line encoding T535P ValRS$^{\Delta}$ led to a profound dominant-negative transformation in cell morphology (Figure 3B). After 24–48 hr of induction, many cells were no longer attached to the culture flask and instead were found floating in the media. While the cells that remain attached appear to retain contact inhibition, and grow as a monolayer, the gapped regions seen between clusters of cells remain prominent over time so that

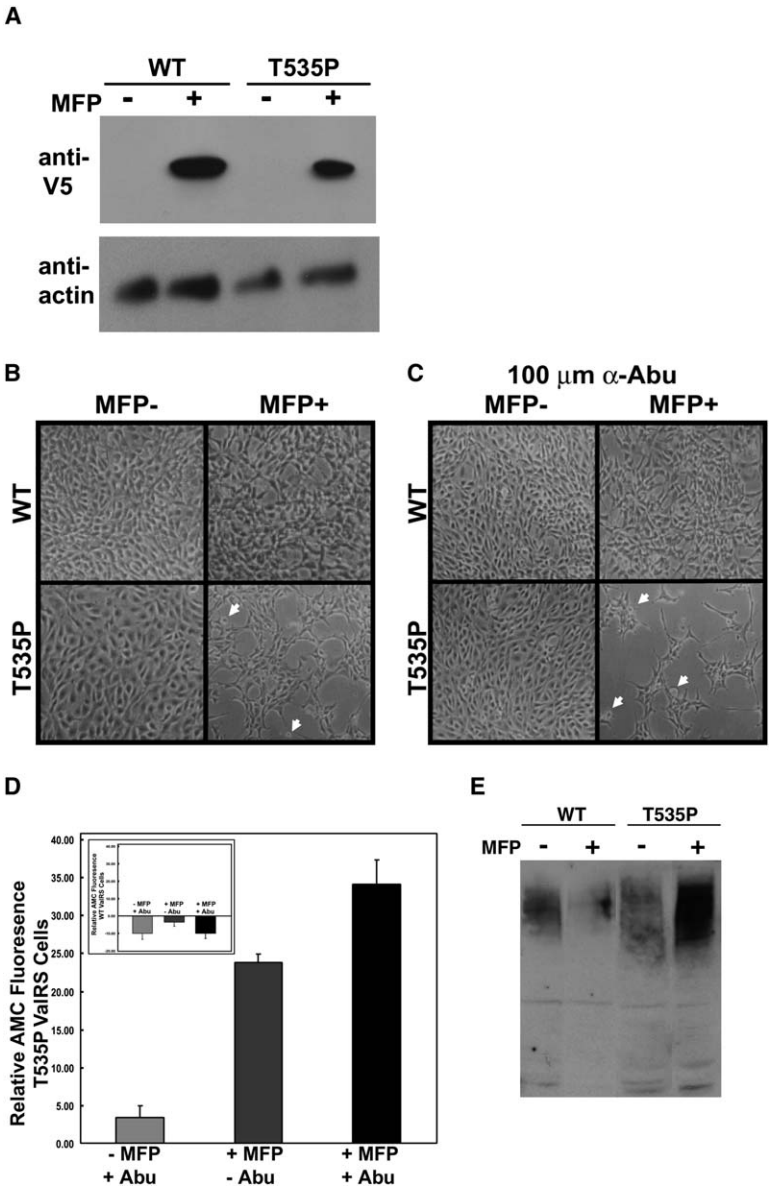

Figure 3. Phenotypic Response to Induction of ValRS$^{\Delta}$ Transgenes

Stably transfected NIH/3T3 cells treated with MFP to induce expression of the WT or T535P ValRS$^{\Delta}$ transgene.

(A) Cell lysates analyzed for transgene expression by immunoblotting with anti-V5-HRP antibody. No basal expression was observed (−MFP).

(B) Phenotypic response of uninduced (−MFP) or induced (+MFP) WT and T535P ValRS$^{\Delta}$ cells grown for 48 hr.

(C) Effects exacerbated in cells expressing T535P ValRS$^{\Delta}$ when cells are grown in α-Abu (100 μM) for 48 hr. White arrows indicate incidences of membrane blebbing, which is indicative of an apoptotic-like response in cells expressing T535P ValRS$^{\Delta}$.

(D) Activation of caspase-3 was observed in cells expressing T535P ValRS$^{\Delta}$, as measured by cleavage of a caspase-3-specific fluorogenic substrate (Ac-DEVD-AMC) when incubated with cell lysates. Increased levels of caspase-3 activation were observed when cells expressing T535P ValRS$^{\Delta}$ were grown in the presence of α-Abu (100 μM) for 24 hr. The fractional difference in fluorescence is relative to assays of uninduced cell lysates. Results are representative of six independent experiments presented as means ± SEM.

(E) Immunoblot of lysates (50 μg) from uninduced (−MFP) or induced (+MFP) WT and T535P ValRS$^{\Delta}$ cells with the anti-polyubiquitin monoclonal antibody.

a confluent monolayer cannot be achieved. Many cells were observed to exhibit altered morphologies characterized by cell contraction and membrane blebbing (as indicated by white arrows). These morphologies are hallmarks of apoptosis. In contrast, induction of the stable cell line encoding wild-type ValRS$^{\Delta}$ caused only a subtle cell-shape change (Figure 3B). Similar phenotypic changes were observed upon induction of full-length wild-type ValRS in a generated stable cell line, showing that the phenotypic effect cannot be attributed to overexpression of truncated ValRS.

To investigate further whether phenotypic differences in cells expressing wild-type versus T535P ValRS$^{\Delta}$ were caused by genetic code ambiguity introduced by errors of aminoacylation, expression in stably transfected NIH/3T3 cell lines was induced in media supplemented with the natural metabolite α-Abu (concentrations ranged from low micromolar to millimolar). ValRS activates α-Abu (K_M elevated ~100-fold in relation to Val) to produce α-Abu-tRNA^{Val} [50] (Figure 3C). Uninduced cells were not visibly affected by the addition of α-Abu (up to 2 mM). As mentioned above, cells expressing wild-type ValRS showed a subtle phenotypic change upon induction. However, no further changes were observed when cells were incubated in media supplemented with α-Abu, up to concentrations of 2 mM. In contrast, the phenotype observed upon induction of T535P ValRS$^{\Delta}$ was exacerbated dramatically by the introduction of α-Abu to the media (Figure 3C). The number of cells remaining attached to the tissue culture dish correlated inversely with the concentration of α-Abu, with the least amount of viable cells present at the highest α-Abu concentrations. Additionally, more numerous incidences of membrane blebbing were observed when cells were treated with α-Abu (white arrows). This striking phenotype demonstrates that, in mammalian cells,

genetic code ambiguity caused by a single point mutation in a specific tRNA synthetase severely affects cell morphology and viability.

Prolonged endoplasmic reticulum stress induced by accumulation of unfolded/misfolded proteins leads to cell death via apoptosis. This process is highlighted by an increase in polyubiquitinylation of the unfolded protein substrates, targeting them for proteosomal degradation. To test whether the apoptotic-like response observed upon induction of T535P ValRS$^{\Delta}$ could be linked to ER stress, cell lysates were immunoblotted with an antibody to specifically detect polyubiquitinylated proteins. Cells expressing T535P ValRS$^{\Delta}$ show a marked increase in polyubiquitinylation compared to uninduced cells and cells expressing wild-type ValRS$^{\Delta}$ (Figure 3E), thus suggesting that an accumulation of misfolded/unfolded proteins may be linked to the apoptotic-like response.

Expression of Editing-Deficient ValRS Induces a Caspase-3-Mediated Apoptotic Response

The execution phase of programmed cell death or apoptosis is characterized by marked changes in cell morphology. One of the most notable of these phenotypic transformations is the effect of membrane blebbing that we observed in cells after induction of T535P ValRS$^{\Delta}$. To explore the link between expression of T535P ValRS$^{\Delta}$ and apoptosis, the activation of caspase-3 (a marker used to identify cells undergoing apoptosis) was investigated. Produced as an inactive zymogen, caspase-3 undergoes proteolytic activation during apoptosis that, in turn, converts the enzyme to a functional cysteine protease [51]. Cleavage by activated caspase-3 was monitored by measuring release of a linked fluorophore upon cleavage of a caspase-3-specific peptide (Ac-DEVD-AMC).

A significant increase in fluorescence resulting from activation of caspase-3 was detected when the fluorogenic peptide was incubated with lysates from induced cells expressing T535P ValRS$^{\Delta}$ compared with lysates from uninduced cells (Figure 3D). Mirroring the trend observed in morphology transformation, when cells expressing T535P ValRS$^{\Delta}$ were treated with α-Abu, the levels of activated caspase-3 increased considerably over those found in induced, untreated cells. In contrast, no significant activation of caspase-3 was observed in induced cells expressing wild-type ValRS$^{\Delta}$ (Figure 3D, inset) compared to uninduced cells, regardless of the presence or absence of α-Abu. Also, when the T535P ValRS$^{\Delta}$ cell line was not induced, but was treated with α-Abu, only a small increase in activated caspase-3 was observed over untreated cells. These results show that genetic code ambiguity in a mammalian cell, induced by the prolonged expression of an editing-deficient ValRS$^{\Delta}$, results in the initiation of an apoptotic response that involves caspase-3 activation. Encouraging increased misincorporation by treatment with α-Abu (a noncognate amino acid that can be misactivated by ValRS) exacerbated this response.

Construction of a Mistranslation-Detecting Sensor

To demonstrate genetic code ambiguity in cells expressing the editing-deficient T535P ValRS$^{\Delta}$, we designed a method to directly monitor the misincorporation of T at V codons. This method was based on the enhanced form of green fluorescent protein (EGFP) from the Pacific Northwest jellyfish *Aequorea victoria*. EGFP has a T at position 65 of its consensus sequence (T-Y-G) that is essential for enhanced fluorescence activity [52–54]. Changes in fluorescence occur upon introduction of substitutions within this consensus sequence. (Substitution of T for wild-type S65 accounts for the enhanced fluorescence and red-shifted excitation maxima of EGFP [55].) We hypothesized that introduction of V65 would alter the fluorescent profile of GFP, allowing detection of misincorporation of T at the position 65 V codon (Figure 4A).

To test this concept, a gene encoding T65V EGFP was transiently transfected into NIH/3T3 cells in culture. In contrast to cells expressing wild-type EGFP, after 48 hr those expressing T65V exhibited, at most, a minimal fluorescent signal (Figures 4B and 4C). Expression of T65V EGFP was verified by immunodetection with a labeled antibody to GFP (Alexa 568-GFP). This result showed that the lack of fluorescence of T65V EGFP was due to elimination of chromophore formation, not to a lack of the presence of mutant protein. (This observation was consistent with the minimal background fluorescent signal also observed in lysates of cells expressing T65V EGFP that were subjected to quantitative analysis of the emission spectra at 509 nm [excitation at 488 nm] [data not shown].) Thus, this system provides a way to monitor T misincorporation as a recovery of fluorescence.

Mistranslation Observed in Cells Expressing Editing-Deficient ValRS

To examine the effects of the ValRS transgenes on Thr misincorporation, the T65V EGFP biosensor was transiently transfected into NIH/3T3 cells stably transfected with inducible forms of either wild-type or T535P ValRS$^{\Delta}$. After T65V transfection (allowing time for cellular recovery), ValRS transgenes were induced and incubated for 12–18 hr to allow for build up of newly synthesized proteins. In cells expressing wild-type ValRS$^{\Delta}$, the minimal T65V EGFP fluorescence did not increase (Figures 5A and 5B). In contrast, cells expressing T535P ValRS$^{\Delta}$ showed a clear gain in EFGP fluorescence (Figures 5A and 5C). This gain is consistent with misincorporation of T at position 65 thereby restoring the chromophore consensus sequence. The presence of comparable amounts of T65V EGFP in cells harboring either the gene for wild-type or T535P ValRS$^{\Delta}$ was confirmed by probing with an antibody to GFP (anti-GFP IgG Alexa Fluor 647). This analysis showed that the increase in EGFP fluorescence resulted from the presence of the editing-defective enzyme, not from an intrinsic difference in levels of EGFP.

To provide a more quantitative measure of fluorescence recovery due to misincorporation, cells were lysed and samples were analyzed for fluorescence emission. In addition, total EGFP fluorescence for each cell sample was corrected for the amount of EGFP protein present. The fractional change in fluorescence was then calibrated by comparing T65V EGFP fluorescence for cells expressing the ValRS$^{\Delta}$ transgenes versus those in which ValRS$^{\Delta}$ transgene expression had not been induced. By using these two standards, a dynamic range of fluorescence emission could be established. This

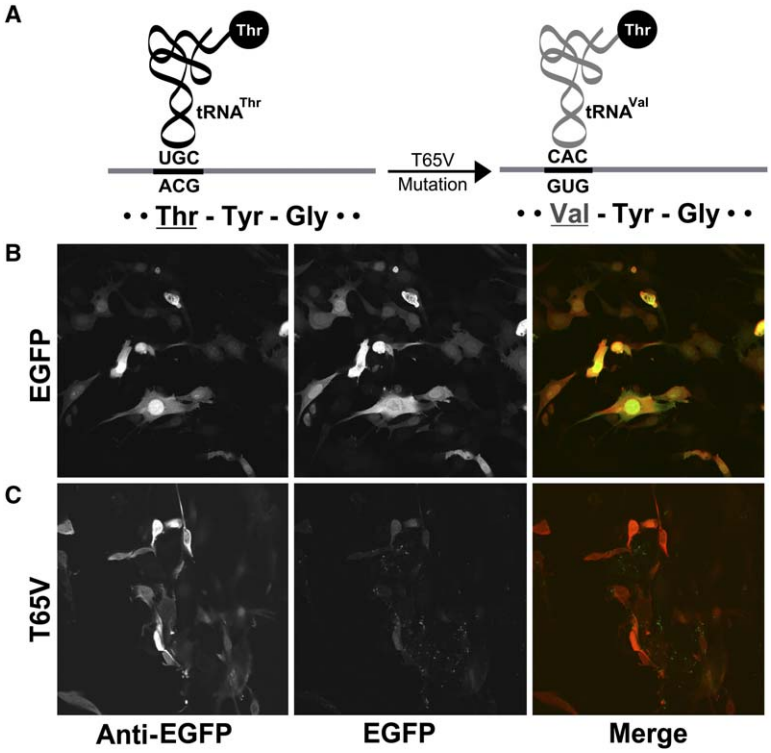

Figure 4. EGFP Biosensor

(A) Schematic of EGFP biosensor. T → V replacement at position 65 of EGFP is hypothesized to alter its fluorescence profile, allowing misincorporation of Thr at V65 (due to the presence of mischarged Thr-tRNA^{Val} generated by an editing-deficient ValRS) to be visualized and measured as the recovery of EGFP fluorescence.

(B and C) Transfection of NIH/3T3 cells with (B) WT and (C) T65V EGFP shows a significant decrease in T65V EGFP fluorescence. Immunodetection with anti-GFP IgG Alexa Fluor 647 illustrates equivalent distribution of both WT and T65V EGFP.

assay demonstrated an ~16.7% ± 1.5% gain in fluorescence in cells coexpressing T535P ValRS$^{\Delta}$ and T65V EGFP, a statistically significant gain (Figure 5A). In contrast, cells expressing wild-type ValRS$^{\Delta}$ did not exhibit a significant quantitative increase in T65V EGFP fluorescence (1.75% ± 2.5%).

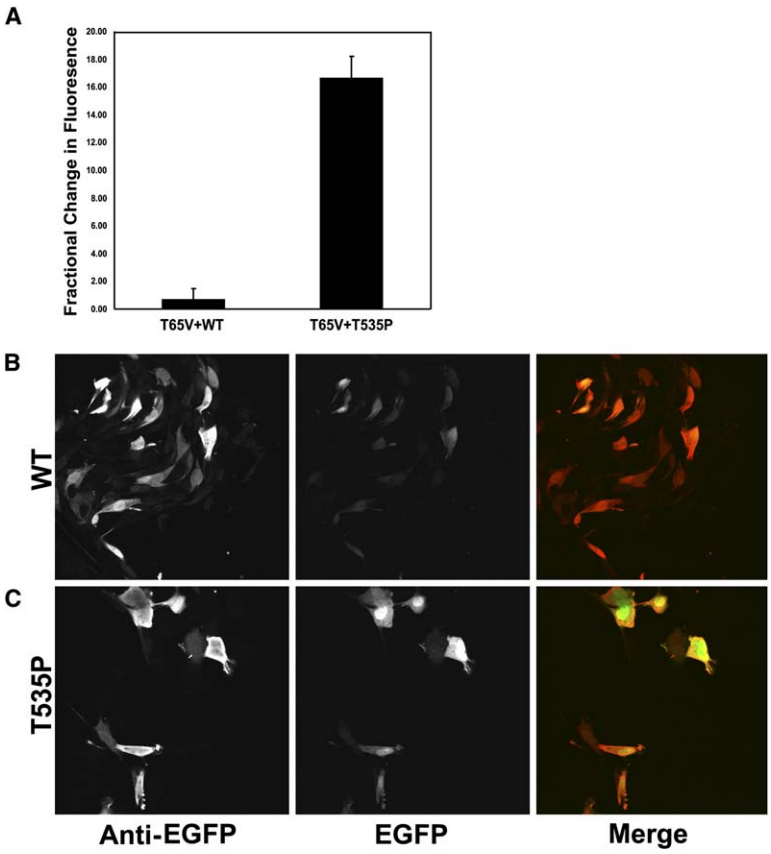

Figure 5. Threonine Misincorporation Detected by EGFP Biosensor

(A–C) NIH/3T3 cells transfected with T65V EGFP and induced to express either WT or T535P ValRS$^{\Delta}$. (A) Fluorescence spectrophotometric analysis of cell lysates (emission at 507 nm; excitation at 488 nm) and visualization by (B and C) fluorescence microscopy demonstrate a gain in EGFP fluorescence in cells expressing (C) T535P, but not (B) WT, ValRS$^{\Delta}$. Emission values were corrected for the amount of EGFP protein present in each sample. The fractional change in fluorescence represents a ratio of the T65V EGFP fluorescence for cells expressing the ValRS$^{\Delta}$ transgenes versus uninduced cells. Results are representative of means of three independent experiments ± SEM.

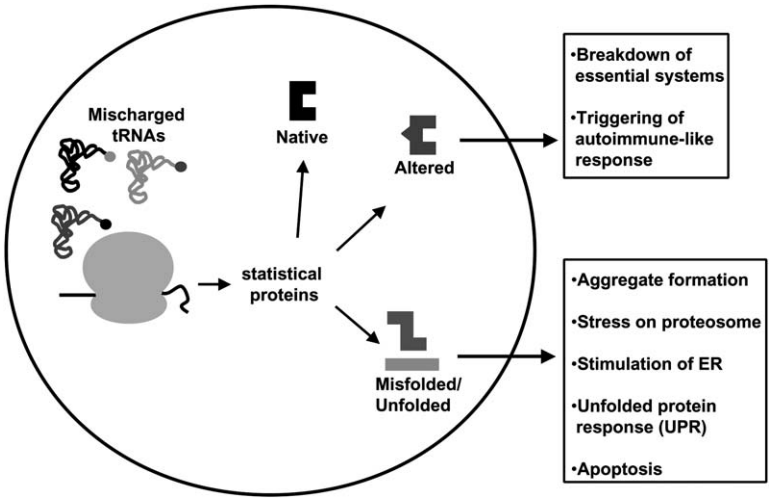

Figure 6. Potential Cellular Impacts of Global Mistranslation

Release of mischarged tRNAs in a eukaryotic cell generated by an editing-deficient aminoacyl-tRNA synthetase and resulting in mistranslation could impact a variety of areas of cell physiology.

In addition to the modified consensus sequence, the EGFP protein contains 18 valines that, when substituted with Thr, may alter the folding or fluorescent properties of EGFP. Possibly, therefore, Val → Thr substitutions at any of these positions could cause local denaturation and exacerbate the loss of fluorescence. To investigate this question, we attempted to "force" substitution of Thr into the other valine codons of EGFP. This attempt was made via raising the exogenous Thr concentration 10-fold. In this extreme circumstance, the fractional gain in T65V fluorescence due to Thr insertion was only slightly reduced (14.4% ± 0.4%, data not shown) compared to the gain in fluorescence without increased Thr (16.7% ± 1.5%). Thus, the effect of the insertion of Thr at sites other than the target site appears to be limited.

Discussion

In comparison to what has been observed in bacteria and yeast, mammalian cells appear to be more sensitive to mistranslation. In *E. coli*, cell viability is only affected in cells in which the wild-type tRNA synthetase allele is knocked out and growth is carried out in the presence of a noncognate amino acid that can be mischarged by the editing-deficient enzyme [14, 15]. In *Candida albicans*, while introduction of ambiguity induces what appears to be a novel stress response (revealed in changes in gene expression and cellular proteome content) that is accompanied by a 50% reduction in growth rate, there is no indication of cell death [56, 57]. In contrast, in mammalian cells, expression of an editing-deficient ValRS is sufficient to cause dramatic changes in cell phenotype and the initiation of an apoptotic response. Because the mutant ValRS studied here acquired the ability to cause amino acid misincorporation, the mutation can be viewed as a gain-of-function mutation. As expected for a gain-of-function mutation, it had a dominant-negative effect over the wild-type alleles.

Previous work showed that when *E. coli* ValRS bearing the corresponding editing mutation (T222P) was introduced into bacteria and grown in the presence of α-Abu, global substitution (mistranslation) at Val codons occurred at a level of up to 24% (as determined by amino acid analysis). For an overexpressed individual protein, the degree of misincorporation for a given peptide ranged between 9.5% and 18% per Val codon (as determined by MALDI-mass spectrometry) [25]. In light of this, it is particularly striking that the fractional gain of 16.7 % in T65V EGFP fluorescence, which was observed in response to an editing-deficient murine ValRS in mammalian cells, falls directly within the range of misincorporation rates observed under similar conditions in bacteria. Although the fractional gain in fluorescence is not considered to directly reflect the level of Thr misincorporation occurring at all Val codons, it has to relate to the degree of Thr misincorporation occurring at Val65 of EGFP. Therefore, this number may loosely reflect the degree of global misincorporation occurring at Val codons when an editing-deficient ValRS is expressed in mammalian cells.

The observed sensitivity of mammalian cells to errors in translation raises the broader question of the mechanistic basis. Through many routes, cell and whole-organism physiology can be impacted by introduction of global changes in primary protein sequence. These routes include disruption of protein folding pathways, creation of altered proteins with newly acquired interactions, or induction of autoimmune-type responses (Figure 6). During the folding process, proteins collapse into their globular native states in a manner determined by their primary amino acid sequence [58, 59]. Thus, small changes in amino acid sequence have the potential to create unfolded polypeptides or misfolded protein aggregates [60, 61]. The appearance of misfolded and/or aggregated proteins in the endoplasmic reticulum (ER) of eukaryotic cells activates a signaling cascade (the unfolded protein response [UPR] [62, 63]) that, when overwhelmed, can lead to cell death via apoptosis [64, 65]. In this scenario, the formation of statistical proteins leads to the initiation of the UPR and induction of an apoptotic response. The accumulation of insoluble protein aggregates is linked to many etiologically unrelated neurodegenerative disorders, pointing to what could be a potential disease-related connection [66–70].

At the organism level, amino acid misincorporation could plausibly trigger an autoimmune-like response. By chemically altering tyrosine residues on the surface

of the native form of thyroglobulin by using arsenillic or sulfanillic acid, Weigle and coworkers demonstrated that, upon injection of the conjugated proteins into rabbits, antibodies formed over time and developed cross-reactivity with their own native thyroglobulin [71, 72]. Prolonged exposure to these self-antibodies resulted in thyroiditis. In principle, this phenomenon can occur when altered proteins are generated by amino acid misincorporation, that is, an immune response provoked in response to altered proteins formed through translational errors could result in the targeting of native proteins and the onset of an autoimmune-like condition.

Sequence alignments demonstrate a high level of conservation in the editing domains of class I tRNA synthetases. In particular, the region into which the T535P mutation was introduced contains some of the most highly conserved residues of the CP1 domain, with key residues conserved in almost every ValRS, IleRS, and LeuRS in organisms ranging from bacteria through humans [32, 33, 73]. Although strict conservation of this sequence throughout evolution shows that strong selective pressure was exerted to retain the editing function, the importance of hydrolytic editing in vivo has only recently been demonstrated in bacteria. The work presented here provides a powerful rationale for this high level of conservation extending to mammals.

Significance

Components of the translation apparatus have been associated with several pathologies and diseases. We have investigated global effects of mistranslation in mammalian cells in culture. AARSs prevent mistranslation through specialized editing reactions that clear any tRNAs that have been aminoacylated with incorrect amino acids. Here, we mutationally disabled the editing function of a murine tRNA synthetase that normally has a potent editing activity. The mutant enzyme is incapable of clearing mischarged tRNA substrates, while, at the same time, it retains wild-type aminoacylation activity. Stable NIH/3T3 mouse fibroblast cell lines were engineered to inducibly express the transgene encoding the mutant enzyme. Prolonged induction of the editing-deficient tRNA synthetase led to a pronounced dominant-negative morphological phenotype. Phenotypic changes were characterized by cell contraction, membrane blebbing, and caspase-3 activation, consistent with an apoptotic-like response. By forcing the use of a noncanonical amino acid that is misacylated and not cleared by the editing-deficient enzyme, morphological effects were exacerbated and activation of caspase-3 was increased. To obtain a direct readout of mistranslation in vivo, a modified EGFP mRNA was expressed, which only produces fluorescent protein when mistranslation occurs. This fluorescent sensor allowed detection of mistranslation upon induction of the editing-deficient tRNA synthetase. In contrast, no fluorescent signal was seen upon induction of the wild-type tRNA synthetase. These investigations show that mistranslation can lead to mammalian cell pathologies and raises the possibility that it has a causal relationship with genetic diseases.

Experimental Procedures

Plasmid Construction

An EST of ~4 kb encoding a putative *M. musculus* ValRS was identified in an EST database (Invitrogen, clone 4971200) by searching against the published sequence [35]. For expression and purification from *E. coli*, the *valS* cDNA from clone 4917200 was subcloned into pET28a (EMD Biosciences) by using SalI and NotI to attach an N-terminal His tag upstream of the *valS* start codon (pLAN410). The QuickChange Site-Directed Mutagenesis Kit (Stratagene) was used to replace the ACC Thr535 codon with a CCC Pro codon (pLAN441). For generation of transgenic cell lines, the coding sequences for wild-type (WT) and T535P ValRS$^{\Delta}$ were subcloned into pGene/V5-His B (Invitrogen) by using HindIII and NotI sites (pLAN438, pLAN443). For misincorporation studies, T65V EGFP was constructed by using site-directed mutagenesis on pEGFP-N1 (BD Clontech) to replace the ACC Thr65 codon with a GUG Val codon.

Molecular Modeling

Sequence of *M. musculus* ValRS containing the editing domain (residues M337–V1137) was submitted for fold recognition to the 3D-PSSM server (http://www.sbg.bio.ic.ac.uk/~3dpssm/). A model was generated by using homology modeling based on the structure of the *T. thermophilus* ValRS editing domain [34]. The model was supported by an E-value of 0.0039, corresponding to confidence in the prediction of >95%. Side chains were modeled in 3D-PSSM by SCWRL.

Aminoacylation and Deacylation Assays

WT and T535P *M. musculus* ValRS were purified from *E. coli* (details are available upon request), and concentrations were determined by the Bradford assay (BioRad) and active site titration. Aminoacylation assays were performed as previously described [22] at 37°C in a reaction mixture of 100 mM HEPES (pH 7.5), 20 mM KCl, 2 mM ATP, 4 mM $MgCl_2$, 2 mM DTT, 20 μM L-valine, 0.7 μM [^{3}H-L-valine], 100 μM calf liver tRNA (EMD Biosciences), and 25 nM WT or T535P ValRS.

Mischarged [^{3}H]-Thr-tRNA^{Val} was generated by incubating *E. coli* T222P ValRS (2 μM), purified *E. coli* tRNA^{Val} (100 μM) (Sigma-Aldrich), and [^{3}H]-L-threonine (20 μM) for 30 min. Deacylation reactions were performed at 25°C in PVDF Multiscreen filter plates (details upon request) with 25 nM enzyme and [^{3}H]-Thr-tRNA^{Val} (11 μM) in 100 mM HEPES (pH7.5), 20 mM KCl, 10 mM $MgCl_2$, and 2 mM DTT. Data points were averaged from duplicate experiments.

Cell Culture

Stably transfected cell lines (GeneSwitch NIH/3T3) were selected, isolated, and maintained in DMEM plus 10% fetal bovine serum, 1% penicillin/streptomycin, 2 mM L-glutamine, 50 μg/ml hygromycin, and 500 μg/ml zeomycin. Lipofectamine and Plus Reagent were used for transfections. ValRS$^{\Delta}$ expression was induced with MFP (1×10^{-8} M) and was detected by immunoblotting with anti-V5-HRP mouse monoclonal antibody (cell culture reagents were purchased from Invitrogen). Monoclonal anti-polyubiquitin antibody, clone FK1 (Biomol), was used to detect polyubiquitinated proteins.

Caspase-3 Activation Assays

Assays measuring caspase-3 activation were performed with the Caspase-3 Assay Kit (BD Pharmingen) according to manufacturer's instructions. Briefly, ValRS$^{\Delta}$ transgenic cell lines were treated with combinations of +/−MFP and α-Abu (100 μM) and were harvested after 24 hr. For each sample, 6×10^6 cells were resuspended in 100 μl lysis buffer for the assay. AMC liberation was measured with a FluoroMax-3 spectrofluorimeter (HORIBA Jobin Yvonn) (excitation at 380 nm; emission at 420–460 nm). The fractional change in fluorescence relative to uninduced cells was determined for each sample. Data represent six independent experiments done in duplicate.

Threonine Misincorporation Assays

WT and T535P ValRS$^{\Delta}$ cell lines were grown to ~60% confluency and transfected with 2 μg pEGFP-N1 (EGFP) or pCMM149 (T65V EGFP)

by using Effectene according to the manufacturer's instructions (QIAGEN). After recovery in growth media (1–2 hr), cells were prepped for either fluorescence microscopy or quantitative analysis.

Fluorescence Microscopy

Cells were seeded onto fibronectin-coated glass coverslips and treated with MFP for 12–18 hr. Cells were then fixed for 20 min in 2% formaldehyde/PBS, permeabilized in 0.2 % Triton X-100/PBS, and rinsed with PBS. Cells were stained with anti-GFP IgG Alexa Fluor 647 conjugate (Molecular Probes) and mounted in immunofluoresence mounting medium (MP Biomedicals). Images were acquired with a Bio-Rad (Zeiss) MRC1024 laser scanning confocal microscope.

Fluorescence Spectrophotometry

Cells were lysed in M-PER Reagent (Pierce), and soluble fractions were isolated. Samples were analyzed with a FluoroMax-3 spectrofluorimeter (HORIBA Jobin Yvonn) (excitation at 488 nm; emission at 507 nm). Units of EGFP per sample were determined by using Amplex Red ELISA kit #1 (Molecular Probes) utilizing an anti-GFP monoclonal antibody, JL-8 (Santa Cruz Biotechnology). HRP was detected by using Amplex Red (excitation at 570 nm; emission at 585 nm), and relative concentrations of EGFP were determined by using a standard curve based on purified EGFP protein standards. Relative EGFP levels were verified by immunoblotting with the same antibody set. Values generated were used to correct for the amount of EGFP protein present in each sample.

Acknowledgments

We thank K. Beebe and B. Cravatt for numerous helpful discussions and advice and for critical reading of the manuscript. We also thank W.B. Kiosses and The Scripps Research Institute Core Microscopy Facility for assistance. L.A.N. was supported by a Norton B. Gilula Graduate Student fellowship and an Achievement Rewards for College Scientists fellowship. This work was supported by grants GM15539 and GM2356 from the National Institutes of Health and by a fellowship from the National Foundation for Cancer Research.

Received: June 20, 2006
Revised: August 28, 2006
Accepted: August 28, 2006
Published: October 20, 2006

References

1. Antonellis, A., Ellsworth, R.E., Sambuughin, N., Puls, I., Abel, A., Lee-Lin, S.Q., Jordanova, A., Kremensky, I., Christodoulou, K., Middleton, L.T., et al. (2003). Glycyl tRNA synthetase mutations in Charcot-Marie-Tooth disease type 2D and distal spinal muscular atrophy type V. Am. J. Hum. Genet. *72*, 1293–1299.
2. Jordanova, A., Irobi, J., and Timmerman, V. (2006). Disrupted function and axonal distribution of mutant tyrosyl-tRNA synthetase in dominant intermediate Charcot-Marie-Tooth neuropathy. Nat. Genet. *38*, 197–202.
3. Lazaris-Karatzas, A., Montine, K.S., and Sonenberg, N. (1990). Malignant transformation by a eukaryotic initiation factor subunit that binds to mRNA 5′ cap. Nature *345*, 544–547.
4. Fukuchi-Shimogori, T., Ishii, I., Kashiwagi, K., Mashiba, H., Ekimoto, H., and Igarashi, K. (1997). Malignant transformation by overproduction of translation initiation factor eIF4G. Cancer Res. *57*, 5041–5044.
5. Zimmer, S.G., DeBenedetti, A., and Graff, J.R. (2000). Translational control of malignancy: the mRNA cap-binding protein, eIF-4E, as a central regulator of tumor formation, growth, invasion and metastasis. Anticancer Res. *20*, 1343–1351.
6. Chambers, D.M., Peters, J., and Abbott, C.M. (1998). The lethal mutation of the mouse wasted (wst) is a deletion that abolishes expression of a tissue-specific isoform of translation elongation factor 1α, encoded by the Eef1a2 gene. Proc. Natl. Acad. Sci. USA *95*, 4463–4468.
7. Shultz, L.D., Sweet, H.O., Davisson, M.T., and Coman, D.R. (1982). 'Wasted', a new mutant of the mouse with abnormalities characteristic to ataxia telangiectasia. Nature *297*, 402–404.
8. Khalyfa, A., Bourbeau, D., Chen, E., Petroulakis, E., Pan, J., Xu, S., and Wang, E. (2001). Characterization of elongation factor-1A (eEF1A–1) and eEF1A–2/S1 protein expression in normal and wasted mice. J. Biol. Chem. *276*, 22915–22922.
9. Leegwater, P.A., Pronk, J.C., and van der Knaap, M.S. (2003). Leukoencephalopathy with vanishing white matter: from magnetic resonance imaging pattern to five genes. J. Child Neurol. *18*, 639–645.
10. Leegwater, P.A., Vermeulen, G., Konst, A.A., Naidu, S., Mulders, J., Visser, A., Kersbergen, P., Mobach, D., Fonds, D., van Berkel, C.G., et al. (2001). Subunits of the translation initiation factor eIF2B are mutant in leukoencephalopathy with vanishing white matter. Nat. Genet. *29*, 383–388.
11. Jakubowski, H., and Goldman, E. (1992). Editing of errors in selection of amino acids for protein synthesis. Microbiol. Rev. *56*, 412–429.
12. Hendrickson, T.L., de Crecy-Lagard, V., and Schimmel, P. (2004). Incorporation of nonnatural amino acids into proteins. Annu. Rev. Biochem. *73*, 147–176.
13. Cochella, L., and Green, R. (2005). Fidelity in protein synthesis. Curr. Biol. *15*, R536–R540.
14. Beebe, K., Ribas De Pouplana, L., and Schimmel, P. (2003). Elucidation of tRNA-dependent editing by a class II tRNA synthetase and significance for cell viability. EMBO J. *22*, 668–675.
15. Nangle, L.A., De Crecy Lagard, V., Doring, V., and Schimmel, P. (2002). Genetic code ambiguity. Cell viability related to the severity of editing defects in mutant tRNA synthetases. J. Biol. Chem. *277*, 45729–45733.
16. Carter, C.W., Jr. (1993). Cognition, mechanism, and evolutionary relationships in aminoacyl-tRNA synthetases. Annu. Rev. Biochem. *62*, 715–748.
17. Lapointe, J., and Giege, R. (1991). Transfer RNAs and aminoacyl-tRNA synthetases. In Translation in Eukaryotes, H. Trachsel, ed. (Boca Raton, FL: CRC Press, Inc.), pp. 35–69.
18. Ibba, M., and Soll, D. (2000). Aminoacyl-tRNA synthesis. Annu. Rev. Biochem. *69*, 617–650.
19. Loftfield, R.B., and Vanderjagt, D. (1972). The frequency of errors in protein biosynthesis. Biochem. J. *128*, 1353–1356.
20. Kurland, C.G. (1992). Translational accuracy and the fitness of bacteria. Annu. Rev. Genet. *26*, 29–50.
21. Baldwin, A.N., and Berg, P. (1966). Transfer ribonucleic acid-induced hydrolysis of valyl-adenylate bound to isoleucyl ribonucleic acid synthetase. J. Biol. Chem. *241*, 839–845.
22. Schreier, A.A., and Schimmel, P.R. (1972). Transfer ribonucleic acid synthetase catalyzed deacylation of aminoacyl transfer ribonucleic acid in the absence of adenosine monophosphate and pyrophosphate. Biochemistry *11*, 1582–1589.
23. Schmidt, E., and Schimmel, P. (1995). Residues in a class I tRNA synthetase which determine selectivity of amino acid recognition in the context of tRNA. Biochemistry *34*, 11204–11210.
24. Yarus, M. (1972). Phenylalanyl-tRNA synthetase and isoleucyl-tRNAPhe; a possible verification mechanism for aminoacyl-tRNA. Proc. Natl. Acad. Sci. USA *69*, 1915–1919.
25. Doring, V., Mootz, H.D., Nangle, L.A., Hendrickson, T.L., de Crecy-Lagard, V., Schimmel, P., and Marliere, P. (2001). Enlarging the amino acid set of *Escherichia coli* by infiltration of the valine coding pathway. Science *292*, 501–504.
26. Bacher, J.M., de Crecy-Lagard, V., and Schimmel, P.R. (2005). Inhibited cell growth and protein functional changes from an editing-defective tRNA synthetase. Proc. Natl. Acad. Sci. USA *102*, 1697–1701.
27. Pezo, V., Metzgar, D., Hendrickson, T.L., Waas, W.F., Hazebrouck, S., Doring, V., Marliere, P., Schimmel, P., and De Crecy-Lagard, V. (2004). Artificially ambiguous genetic code confers growth yield advantage. Proc. Natl. Acad. Sci. USA *101*, 8593–8597.
28. Lee, J.W., Beebe, K., Nangle, L.A., Jang, J., Longo-Guess, C., Cook, S.A., Davisson, M.T., Sundberg, J.P., Schimmel, P., and Ackerman, S.L. (2006). Editing-defective tRNA synthetase causes protein misfolding and neurodegeneration in the sticky mouse. Nature *443*, 50–55.
29. Lin, L., and Schimmel, P. (1996). Mutational analysis suggests the same design for editing activities of two tRNA synthetases. Biochemistry *35*, 5596–5601.
30. Nureki, O., Vassylyev, D.G., Tateno, M., Shimada, A., Nakama, T., Fukai, S., Konno, M., Hendrickson, T.L., Schimmel, P., and

Yokoyama, S. (1998). Enzyme structure with two catalytic sites for double-sieve selection of substrate. Science *280*, 578–582.

31. Silvian, L.F., Wang, J., and Steitz, T.A. (1999). Insights into editing from an Ile-tRNA synthetase structure with $tRNA^{Ile}$ and mupirocin. Science *285*, 1074–1077.
32. Mursinna, R.S., Lee, K.W., Briggs, J.M., and Martinis, S.A. (2004). Molecular dissection of a critical specificity determinant within the amino acid editing domain of leucyl-tRNA synthetase. Biochemistry *43*, 155–165.
33. Hendrickson, T.L., Nomanbhoy, T.K., de Crecy-Lagard, V., Fukai, S., Nureki, O., Yokoyama, S., and Schimmel, P. (2002). Mutational separation of two pathways for editing by a class I tRNA synthetase. Mol. Cell *9*, 353–362.
34. Fukunaga, R., and Yokoyama, S. (2005). Structural basis for non-cognate amino acid discrimination by the valyl-tRNA synthetase editing domain. J. Biol. Chem. *280*, 29937–29945.
35. Snoek, M., and Van Vugt, H. (1999). The sequence and organization of the mouse valyl-tRNA synthetase gene G7a/Bat6 located in the MHC class III region. Immunogenetics *49*, 468–470.
36. Fischer, D., Barret, C., Bryson, K., Elofsson, A., Godzik, A., Jones, D., Karplus, K.J., Kelley, L.A., MacCallum, R.M., Pawowski, K., et al. (1999). CAFASP-1: critical assessment of fully automated structure prediction methods. Proteins (*Suppl 3*), 209–217.
37. Kelley, L.A., MacCallum, R.M., and Sternberg, M.J. (2000). Enhanced genome annotation using structural profiles in the program 3D-PSSM. J. Mol. Biol. *299*, 499–520.
38. Dunbrack, R.L., Jr. (1999). Comparative modeling of CASP3 targets using PSI-BLAST and SCWRL. Proteins (*Suppl 3*), 81–87.
39. Roy, H., Ling, J., Alfonzo, J., and Ibba, M. (2005). Loss of editing activity during the evolution of mitochondrial phenylalanyl-tRNA synthetase. J. Biol. Chem. *280*, 38186–38192.
40. Hsieh, H.L., and Campbell, D.R. (1991). Evidence that gene G7a in the human major histocompatibility complex encodes valyl-tRNA synthetase. Biochem. J. *278*, 809–816.
41. Godar, D.E., and Yang, D.C. (1988). Mammalian high molecular weight and monomeric forms of valyl-tRNA synthetase. Biochemistry *27*, 2181–2186.
42. Vilalta, A., Donovan, D., Wood, L., Vogeli, G., and Yang, D.C. (1993). Cloning, sequencing and expression of a cDNA encoding mammalian valyl-tRNA synthetase. Gene *123*, 181–186.
43. Bec, G., and Waller, J.P. (1989). Valyl-tRNA synthetase from rabbit liver. II. The enzyme derived from the high-Mr complex displays hydrophobic as well as polyanion-binding properties. J. Biol. Chem. *264*, 21138–21143.
44. Bec, G., Kerjan, P., and Waller, J.P. (1994). Reconstitution in vitro of the valyl-tRNA synthetase-elongation factor (EF) 1 beta gamma delta complex. Essential roles of the NH2-terminal extension of valyl-tRNA synthetase and of the EF-1 delta subunit in complex formation. J. Biol. Chem. *269*, 2086–2092.
45. Chatton, B., Walter, P., Ebel, J., Lacroute, F., and Fasiolo, F. (1988). The yeast *VAS1* gene encodes both mitochondrial and cytoplasmic valyl-tRNA synthetases. J. Biol. Chem. *263*, 52–57.
46. Negrutskii, B.S., Shalak, V.F., Kerjan, P., El'skaya, A.V., and Mirande, M. (1999). Functional interaction of mammalian Valyl-tRNA synthetase with elongation factor EF-1α in the complex with EF-1H. J. Biol. Chem. *274*, 4545–4550.
47. Motorin, Y.A., Wolfson, A.D., Lohr, D., Orlovsky, A.F., and Gladilin, K.L. (1991). Purification and properties of a high-molecular-mass complex between Val-tRNA synthetase and the heavy form of elongation factor 1 from mammalian cells. Eur. J. Biochem. *201*, 325–331.
48. Bec, G., Kerjan, P., Zha, X.D., and Waller, J.P. (1989). Valyl-tRNA synthetase from rabbit liver. I. Purification as a heterotypic complex in association with elongation factor 1. J. Biol. Chem. *264*, 21131–21137.
49. Park, S.G., Kim, H.J., Min, Y.H., Choi, E.C., Shin, Y.K., Park, B.J., Lee, S.W., and Kim, S. (2005). Human lysyl-tRNA synthetase is secreted to trigger proinflammatory response. Proc. Natl. Acad. Sci. USA *102*, 6356–6361.
50. Jakubowski, H., and Fersht, A.R. (1981). Alternative pathways for editing non-cognate amino acids by aminoacyl-tRNA synthetases. Nucleic Acids Res. *9*, 3105–3117.
51. Nicholson, D.W., Ali, A., Thornberry, N.A., Vaillancourt, J.P., Ding, C.K., Gallant, M., Gareau, Y., Griffin, P.R., Labelle, M., and Lazebnik, Y.A. (1995). Identification and inhibition of the ICE/CED-3 protease necessary for mammalian apoptosis. Nature *376*, 37–43.
52. Cormack, B.P., Valdivia, R.H., and Falkow, S. (1996). FACS-optimized mutants of the green fluorescent protein (GFP). Gene *173*, 33–38.
53. Prasher, D.C., Eckenrode, V.K., Ward, W.W., Prendergast, F.G., and Cormier, M.J. (1992). Primary structure of the *Aequorea victoria* green-fluorescent protein. Gene *111*, 229–233.
54. Cody, C.W., Prasher, D.C., Westler, W.M., Prendergast, F.G., and Ward, W.W. (1993). Chemical structure of the hexapeptide chromophore of the *Aequorea* green-fluorescent protein. Biochemistry *32*, 1212–1218.
55. Heim, R., Cubitt, A., and Tsien, R. (1995). Improved green fluorescence. Nature *373*, 663–664.
56. Santos, M.A., Cheesman, C., Costa, V., Moradas-Ferreira, P., and Tuite, M.F. (1999). Selective advantages created by codon ambiguity allowed for the evolution of an alternative genetic code in *Candida spp*. Mol. Microbiol. *31*, 937–947.
57. Santos, M.A., Ueda, T., Watanabe, K., and Tuite, M.F. (1997). The non-standard genetic code of *Candida spp.*: an evolving genetic code or a novel mechanism for adaptation? Mol. Microbiol. *26*, 423–431.
58. Gething, M., and Sambrook, J. (1992). Protein folding in the cell. Nature *355*, 33–45.
59. Anfinsen, C.B. (1973). Principles that govern folding of protein chains. Science *181*, 223–230.
60. Gow, A., and Sharma, R. (2003). The unfolded protein response in protein aggregating diseases. Neuromolecular Med. *4*, 73–94.
61. Cohen, F.E., and Kelly, J.W. (2003). Therapeutic approaches to protein-misfolding diseases. Nature *426*, 905–909.
62. Forman, M.S., Lee, V.M., and Trojanowski, J.Q. (2003). 'Unfolding' pathways in neurodegenerative disease. Trends Neurosci. *26*, 407–410.
63. Kaufman, R.J. (2002). Orchestrating the unfolded protein response in health and disease. J. Clin. Invest. *110*, 1389–1398.
64. Bence, N.F., Sampat, R.M., and Kopito, R.R. (2001). Impairment of the ubiquitin-proteasome system by protein aggregation. Science *292*, 1552–1555.
65. Perlmutter, D.H. (2002). The cellular response to aggregated proteins associated with human disease. J. Clin. Invest. *110*, 1219–1220.
66. Trojanowski, J.Q. (2002). Tauists, Baptists, Syners, Apostates, and new data. Ann. Neurol. *52*, 263–265.
67. Bucciantini, M., Giannoni, E., Chiti, F., Baroni, F., Formigli, L., Zurdo, J., Taddei, N., Ramponi, G., Dobson, C.M., and Stefani, M. (2002). Inherent toxicity of aggregates implies a common mechanism for protein misfolding diseases. Nature *416*, 507–511.
68. Aridor, M., and Balch, W.E. (1999). Integration of endoplasmic reticulum signaling in health and disease. Nat. Med. *5*, 745–751.
69. Yankner, B.A., Duffy, L.K., and Kirschner, D.A. (1990). Neurotrophic and neurotoxic effects of amyloid β protein: reversal by tachykinin neuropeptides. Science *250*, 279–282.
70. Koo, E.H., Lansbury, P.T., Jr., and Kelly, J.W. (1999). Amyloid diseases: abnormal protein aggregation in neurodegeneration. Proc. Natl. Acad. Sci. USA *96*, 9989–9990.
71. Weigle, W.O. (1965). The induction of autoimmunity in rabbits following injection of heterologous or altered homologous thyroglobulin. J. Exp. Med. *121*, 289–308.
72. Weigle, W.O. (1962). Termination of acquired immunological tolerance to protein antigens following immunization with altered protein antigens. J. Exp. Med. *116*, 913–928.
73. Ribas de Pouplana, L., and Schimmel, P. (2001). Formation of two classes of tRNA synthetases in relation to editing functions and genetic code. Cold Spring Harb. Symp. Quant. Biol. *66*, 131–166.